

# UCSF

## UC San Francisco Previously Published Works

### Title

Monitoring silver diamine fluoride application with optical coherence tomography and thermal imaging: An in vitro proof of concept study

### Permalink

<https://escholarship.org/uc/item/0cq320qj>

### Journal

Lasers in Surgery and Medicine, 54(5)

### ISSN

1050-9267

### Authors

Abdelaziz, Marwa

Yang, Vincent

Chang, Nai-Yuan Nicholas

et al.

### Publication Date

2022-07-01



### DOI

10.1002/lsm.23528

Peer reviewed

**BASIC SCIENCE**

# Monitoring silver diamine fluoride application with optical coherence tomography and thermal imaging: An in vitro proof of concept study

Marwa Abdelaziz DMD, PhD<sup>1,2</sup>  | Vincent Yang BS<sup>1</sup> |  
Nai-Yuan Nicholas Chang DDS<sup>1</sup> | Cynthia Darling PhD<sup>1</sup> | William Fried BS<sup>1</sup> |  
Jong Seto PhD<sup>1</sup> | Daniel Fried PhD<sup>1</sup> 

<sup>1</sup>Department of Preventive and Restorative Dental Science, UCSF, San Francisco, California, USA

<sup>2</sup>Division of Cariology and Endodontics, University of Geneva, Geneva, Switzerland

**Correspondence**

Marwa Abdelaziz, DMD, PhD, Department of Preventive Dental Medicine and Primary Dental Care, Division of Cariology and Endodontology, University Clinics of Dental Medicine (CUMD), Faculty of Medicine, University of Geneva, 1 rue Michel-Servet CH-1211, Switzerland.  
Email: [marwa.abdel@unige.ch](mailto:marwa.abdel@unige.ch)

**Funding information**

NIH, Grant/Award Numbers: F30-DE027264., R01-DE027335; Schweizerischer Nationalfonds zur Förderung der Wissenschaftlichen Forschung, Grant/Award Number: P2GEP3\_188157

**Abstract**

**Objectives:** The purpose of this study was to show that optical coherence tomography (OCT) and thermal imaging can be used to monitor changes in the structure and activity of caries lesions over time after treatment with silver diamine fluoride (SDF).

**Methods:** Artificial caries lesions were formed on enamel and dentin bovine blocks. Each block was partitioned into five windows with the central three windows exposed to a demineralization solution to create lesions: one sound window served as a sound control (SC), one sound window was exposed to SDF to serve as a test control (SCT), one lesion window served as a lesion control (LC), one lesion window received one application of SDF (L1), while the other lesion window received two applications of SDF (L2). Each window was scanned using OCT before SDF application, and every week subsequently, for 12 weeks after initial SDF treatment. Changes in the mean intensity and the width of the peak of increased reflectivity due to the lesion and SDF along with the intensity at a depth of 180  $\mu\text{m}$  from the surface representing optical penetration through the lesion were monitored. Changes in the heat lost,  $\Delta Q$  (temperature integrated over time) of each window during drying with air were also monitored using a thermal imaging camera. Transverse microradiography (TMR), and high-resolution microscopy were also used for the analysis of selected samples.

**Results:** The reflectivity and optical penetration of sound and lesion areas of enamel and dentin manifested significant changes in OCT images after SDF application. Thermal imaging showed significant differences in  $\Delta Q$  indicative of permeability changes in the sound and lesion areas of enamel and dentin after SDF application.

**KEYWORDS**

caries, monitoring lesion activity, OCT, optical coherence tomography, SDF, silver diamine fluoride, thermal imaging

## INTRODUCTION

In the effort to prevent new caries lesions and arrest already formed lesions, several products with anticaries properties and higher fluoride concentrations were introduced over the years. Silver diamine fluoride (SDF) combines the antibacterial effects of silver and the remineralizing effects of fluoride.

The first report concerning the use of silver to arrest carious lesions was published by Stebbins in 1891, he used silver nitrate to affect the dental caries of his patients.<sup>1</sup> Since then many different silver salt preparations have been used to control carious lesions. The Western Australia Dental Service used silver fluoride (AgF) for disadvantaged children and was successful in inhibiting the growth of existing lesions. Many of the past decade's papers reported various times of applications and success rates.<sup>2</sup> Many of these studies were anecdotal but the reports stated that there was a significant reduction in the progress of the lesions. SDF was mainly used in pediatric dental practices. A recent randomized clinical trial showed a success rate of 66.9% for annual application and 75.7% for semiannual application.<sup>3</sup> All this makes SDF a promising therapeutic agent for the noninvasive management of caries lesions. SDF has become widely available after FDA approval as a desensitizing agent in the United States.<sup>4</sup>

SDF (Advantage Arrest; Elevate Oral Care, LLC) is a colorless liquid containing silver fluoride ions that at pH 10 is composed of 25% silver, 8% ammonia, 5% fluoride, and 62% water. This is referred to as 38% SDF (containing 44,800 ppm fluoride). SDF's ability to halt the caries process and to simultaneously prevent the formation of new caries makes SDF different from other caries-preventive agents, such as sodium fluoride (5%) and stannous fluoride (2%–8%).<sup>5</sup> Clinical trials reported the successful use of SDF to arrest coronal caries<sup>6</sup> and a meta-analysis found that the overall caries arrest rate for SDF was 81%.<sup>2</sup> Ex vivo studies demonstrated that SDF increased the microhardness and mineral density of the caries lesions.<sup>7,8</sup> SDF has also been found to inhibit the growth of cariogenic bacteria and the formation of cariogenic biofilm.<sup>9,10</sup> The treatment effectiveness in vivo is approximately 68% (range 31%–79%).<sup>2,4,5</sup>

This noninvasive and efficient caries-arresting capability of SDF has drawn much attention from dental clinicians and researchers. The effect of SDF has been assessed in different ways in various in vitro studies. Properties of SDF treated teeth such as mineral density, elemental contents, surface morphology, and crystal characteristics were assessed by microcomputed tomography (micro-CT), energy-dispersive X-ray spectrometry (EDX), scanning electron microscopy (SEM), transverse microradiography (TMR), transmission electron microscopy (TEM), and atomic absorption spectrometry (AAS).<sup>7,11</sup> However, these methods are laboratory-based and cannot be performed clinically. In

clinical studies, clinical observation of the lesion appearance and its resistance to probing have served to show that lesions remain arrested after SDF application.

OCT enables accurate, real-time evaluation of changes in lesion structure with high resolution. It is a non-invasive and non-destructive diagnostic method, that uses nonionizing short-wavelength infrared (SWIR) light with high sensitivity and specificity for the detection and monitoring of early lesions.<sup>12–15</sup> OCT has been used successfully to measure demineralization and remineralization in vitro in simulated caries models in dentin and on root surfaces.<sup>16–18</sup> OCT has also been explored to monitor remineralization on enamel and dentin surfaces and to detect the formation of a highly mineralized layer on the lesion surface after exposure to a remineralization solution.<sup>18</sup> OCT has also been used for several in vivo studies to detect and monitor caries lesions and monitor demineralization and remineralization.<sup>19–23</sup>

The lack of a mechanistic understanding of the activity of SDF in arresting caries has hindered its use in the clinic and has led to large variations in treatment. Previous studies showed that silver and fluoride ions penetrate ~25  $\mu\text{m}$  into the enamel, and 50–200  $\mu\text{m}$  into dentin.<sup>8</sup> In another work, SDF arrested lesions were measured to be 150  $\mu\text{m}$  thick.<sup>7</sup> The need for reapplying SDF is still not fully understood, some sources suggest once-a-year application while others suggest bi-annual application.<sup>4</sup> In another paper, three applications of SDF within 6 weeks led to the arrest of rampant caries in a young teenager.<sup>24</sup> The arrested caries lesions were coal-black in appearance and were hard to probe after treatment. Without proper tools to monitor the effect of SDF over time, suggestions for reapplication are solely based on subjective observations of clinicians. Real-time clinical monitoring is needed to monitor changes in lesions over time after treatment.

The high imaging speed of OCT measurements is aptly suited for the many clinical requirements in detecting dental caries, including use for early diagnosis and monitoring lesion progression.

Natural caries lesion arrest is accompanied by remineralization in the outer surface layers of the lesion. The higher mineral content of the outer zone inhibits the diffusion of fluids between the surface and the bulk of the lesion. The rate of water diffusion out of the lesion reflects the degree of lesion activity. The loss of water from the porous lesion can change the reflectivity and the scattering of light from the lesion and studies have demonstrated that the optical changes due to the loss of water from porous lesions can be used to assess lesion's activity with fluorescence and SWIR imaging.<sup>25–28</sup> Several studies have shown that thermal imaging can be used to detect changes in tooth mineralization. Kaneko et al. and Zakian et al.<sup>29,30</sup> demonstrated that lesions on coronal surfaces could be differentiated from sound enamel in thermal images. Later studies showed that temperature changes due to the loss of water from porous lesions can

also be used to assess lesion activity using thermal imaging.<sup>26–28</sup> In those previous studies, thermal imaging during lesion dehydration was more successful than SWIR imaging for assessing lesion activity on root and dentin surfaces.<sup>28</sup> Recently, the first clinical study was carried out demonstrating that thermal imaging can be used to assess the activity of root caries lesions.<sup>31</sup>

The surface zone formed during remineralization in an arresting caries lesion correlates directly to properties of permeability and activity in the lesion. When correlated with results from SWIR imaging during dehydration measurements and OCT measurements, it was found that minor changes in surface layer thickness may lead to significant changes in fluid permeability in remineralized lesions.<sup>28</sup>

Initial studies suggest that the application of SDF leads to lesion arrest by forming a highly mineralized layer on the lesion surface as a result of the reaction of silver and fluoride with the hydroxyapatite of the tooth structure.<sup>32</sup> Other work has described the formation of silver microwires that plug the dentine tubules and reinforce the demineralized lesion structure.<sup>33</sup>

This paper investigates the treatment of caries lesions with SDF in vitro utilizing two non-destructive optical-based methods, optical coherence tomography (OCT) and thermal imaging.

These tools will likely increase our understanding of the mechanism of action of SDF in reducing lesion activity and help develop more effective treatment protocols. To achieve this, we look at changes occurring over time in the reflectivity, optical penetration (OP), and the permeability of simulated lesions treated with SDF.

## MATERIALS AND METHODS

### Sample preparation

Forty-six enamel and dentin blocks of approximately 10–12 mm in length with a width of 2 mm and a thickness of 2–4 mm were prepared from extracted bovine incisors acquired from a slaughterhouse. It is much easier to generate consistent simulated lesions on bovine enamel than on human extracted teeth. Human teeth are exposed to varying amounts of fluoride and many teeth are highly resistant to demineralization. Many cariology studies have utilized bovine enamel to study demineralization and remineralization including several of the referenced SWIR and OCT studies.<sup>12,14,34</sup> The enamel and dentin blocks were mounted on a resin block to facilitate further manipulation. The surfaces of the bovine blocks were ground to a 9 µm finish to obtain a flat surface. Each sample was partitioned into five regions or windows (one sound control, three lesions, and one test control) by etching small incisions 2 mm apart across each of the blocks using a laser. Incisions were etched using an RF-excited laser, Diamond J5-V from Coherent operating at

a wavelength of 9.3 µm with a pulse duration of 26 microseconds and a pulse repetition rate of 200 Hz. The laser beam was focused to a beam diameter of 200 µm using a ZnSe lens of 100 mm focal length. The incident fluence was 30 J/cm<sup>2</sup>. An air-actuated fluid spray delivery system consisting of a 780 S spray valve, a Valvemate 7040 controller, and a water reservoir from EFD, Inc. was used to provide a continuous and uniform spray of fine water mist (5 ml/mm) onto sample surfaces to prevent thermal damage to the samples.

Lesion areas (three central windows) were subjected to demineralization using a surface softened lesion model, one that produces subsurface demineralization without erosion of the surface.<sup>35</sup> A thin layer of acid-resistant varnish in the form of nail polish, Revlon, was applied to protect the sound and test control windows before exposure to the demineralization solution. The enamel samples (*N* = 26) were immersed in 45 ml aliquots of the demineralization solution for 48 hours. The mineral loss profiles are fairly uniform in these lesions and they emulate an active lesion. The lesions produced were approximately 80–100 µm deep. The demineralization solution, which was maintained at 37°C and pH 4.7, was composed of 2.0 mmol/L calcium, 2.0 mmol/L phosphate, and 0.075 mol/L acetate. After the demineralization period, the acid-resistant varnish was removed from the sound test window and then was applied again to the sound control and lesion control windows. For the dentin blocks (*N* = 20), the same demineralization protocol was performed, however, the pH of the demineralization solution was adjusted to 4.9.

Finally, each block had the following five windows as shown in Figure 1. SC: sound control covered with nail varnish. LC: lesion control covered with nail polish. L1: lesion that received one SDF application (Week 0). L2: lesion that received two SDF applications (Week 0 and Week 6).

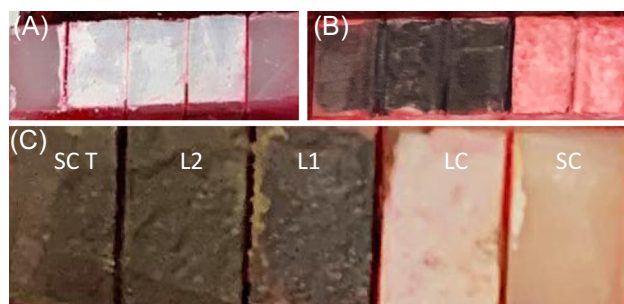


**FIGURE 1** Images of the enamel block after lesion preparation (A), and after SDF application showing the dark precipitation of silver on the surface on the exposed windows and the red nail varnish on the protected windows (B). And final situation (C) after two applications showing all windows after nail varnish removal. L1, one SDF application (Week 0); L2, two SDF applications (Week 0 and Week 6); LC, lesion control; SC, sound control; SCT, sound control that received two SDF applications (Week 0 and Week 6); SDF, silver diamine fluoride

SCT: sound control that received two SDF applications (Week 0 and Week 6).

## SDF application and storage in artificial saliva

Silver Diamine Fluoride 38% (Advantage Arrest™; Elevate Oral Care) was applied to the two exposed lesions and the sound test windows following the protocol developed at the University of California, San Francisco (UCSF) for SDF.<sup>4</sup> The SDF product was applied on a dried surface using a microbrush, left to dry for a minute before storing the blocks in an artificial saliva solution (pH 7) at 37°C. The solution was composed of 1.5 mmol/L calcium, 0.9 mmol/L phosphate, 150 mmol/L KCl, and 20 mmol/L HEPES buffer maintained at pH 7.0°C and 37°C. After 6 weeks from the first application, SDF was reapplied on one of the windows (L2) and the sound test window (SCT).

## OCT imaging

A Santec IVS-2000-HR-C OCT (Komaki) was used for the OCT imaging measurements. This system utilizes a swept laser source and a handpiece with a microelectromechanical (MEMS) scanning mirror and imaging optics. It is capable of acquiring complete tomographic images with a volume of  $5 \times 5 \times 5$  mm in approximately 3 seconds. The body of the handpiece is  $7 \times 18$  cm with an imaging tip that is 4 cm long and 1.5 cm across. This system operates at a wavelength of 1312 nm with a bandwidth of 173 nm with a measured axial resolution in air of  $8.8 \mu\text{m}$  (3 dB). This translates to axial resolutions of 5.5 and  $6.1 \mu\text{m}$  in enamel and dentin, respectively after correcting for the refractive index. The lateral resolution is  $30 \mu\text{m}$  ( $1/e^2$ ) with a transverse imaging window of  $5 \text{ mm} \times 5 \text{ mm}$  and a measured imaging depth of 5 mm in air. The exposed windows on the tooth samples were imaged before application of SDF and then at weeks 1, 2, 3, 4, 6, 7, 8, 10 after application. After 12 weeks the nail polish was removed from the sound control and lesion control and all windows were imaged. In this study, to suppress strong specular reflection and surface scattering from the flat sample surfaces, we applied a thin layer of glycerol on the surface of the samples.<sup>36</sup> It was applied with an optical wipe and was not allowed to pool on the surface. It does not interfere with measurement of the subsurface structure or measurement of the lesion depth. It is water-soluble and easy to remove.

Each OCT image for each sample window was analyzed by averaging the point scans (a-scans) across the entire window (b-scan), generating a smoothed average intensity curve through the depth of the sample window using MATLAB (MathWorks). The width of the high-intensity peak (PW) representing the increased reflectivity at the sample surface (specular reflection) and

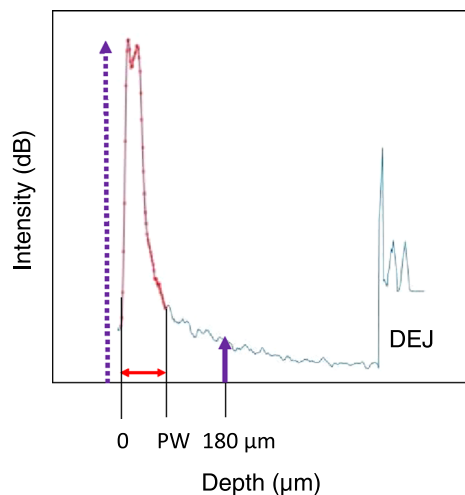


**FIGURE 2** A depth versus intensity curve (OCT a-scan) measured on an OCT b-scan obtained from a lesion window on one of the bovine enamel samples before the application of SDF. The large peak in the curve represents the increased reflectivity from the lesion. The peak width (PW) is represented by the double red arrow. The mean intensity is represented by the integrated intensity over the lesion depth, the blue shaded area under the peak. The intensity of  $180 \mu\text{m}$  below the surface representing the optical penetration through the lesion was also monitored. The second peak is the dental enamel junction (DEJ). OCT, optical coherence tomography; SDF, silver diamine fluoride

from the lesion was monitored over time along with the mean intensity integrated over that width (PW) as shown in Figure 2. In addition, the intensity at a depth of  $180 \mu\text{m}$  below the surface was also monitored over time since this measurement reflects the OP through the sample surface and through the entire lesion ( $\sim 100 \mu\text{m}$  thick).

## Thermal imaging

A custom thermal imaging dehydration setup was used to monitor changes in sample surface temperature during dehydration.<sup>26–28</sup> Each sample was placed in a mount connected to a high-speed XY-scanning motion controller system (Newport) ESP301 controller and 850G-HS stages, coupled with an air nozzle and thermal camera. After the sample was removed from the water bath at 20°C, it was immediately dried with a stream of air from the air nozzle. The airstream pressure was set to 15 psi and the computer-controlled air nozzle was positioned 5 cm away from the sample. Each measurement consisted of capturing a sequence of images at 4 frames per second for 40 seconds. The dehydration setup was completely automated using LabVIEW software (National Instruments) and programmed to begin drying after 3 seconds of imaging to obtain a baseline measurement.

An infrared (IR) thermography camera, Model A65 (FLIR Systems) sensitive from 8 to  $13 \mu\text{m}$  with a

resolution of  $640 \times 512$  pixels, thermal sensitivity of 50 mK, and a lens with a 13 mm focal length was used to record temperature changes during the dehydration process. The exposed windows on the samples were imaged before application of SDF and then at weeks 1, 2, 3, 4, 6, 7, 8, 10 after application. After 12 weeks the nail polish was removed from the sound control and lesion control and all windows were imaged. For each sample region/window, a region of interest (ROI) was designated and the mean intensity of pixels in each ROI was monitored over time during drying to generate plots of temperature profiles over time.

Typical measurements reveal thermal profiles to have a sharp dip in intensity, followed by a gradual asymptotic growth to a final intensity level. This behavior corresponds to the evaporation of water, cooling of the surface of the tooth, and then gradual recovery to ambient temperature. We call the overall energy lost from the lesion area due to evaporative cooling,  $\Delta Q$ . The area under the curve (temperature integrated over time) from the time in which it dips below the initial temperature to the time that it rises above the initial temperature was used to calculate  $\Delta Q$ . In Figures 1 and 7, this is the area below the gray line. Changes in  $\Delta Q$  on each region/window over time were measured and repeated measures analysis of variance (ANOVA) was used to detect significant changes over time. The  $\Delta Q$  values on the 5 windows were also compared for Week 12. Statistical analyses were carried out using GraphPad Prism 9.0.

### Transverse microradiography (TMR)

A custom-built digital (TMR) system was used to measure mineral loss in the selected samples ( $N = 5$ ). A high-speed motion control system with Newport UTM150 and 850 G stages and an ESP300 controller coupled to a video microscopy and laser targeting system was used for precise positioning of the tooth samples in the field of view of the imaging system. Line profiles were taken from TMR images of thin cross-sections, with a thickness of 200  $\mu\text{m}$ , cut along the same position scanned by OCT. X-ray attenuation was converted to volume percent mineral using a calibration curve as performed previously.<sup>37</sup> The TMR images were converted from 12-bit intensity values representing X-ray attenuation through the thin section, to volume % mineral using a calibration plot and the section thickness. The line-profiles were integrated to a depth of 200  $\mu\text{m}$  and subtracted from a line profile taken of a sound area from the same tooth to yield the integrated mineral loss or the  $\Delta Z$  value ( $\text{vol.}\% \times \mu\text{m}$ ) that is typically used in cariology research that represents the overall severity of the caries lesion. Since there was cavitation in some samples, we substituted 20% mineral for the missing areas. The integrations were performed using Igor Pro software (Wavemetrics). Significant differences among sample

groups were determined using repeated-measures ANOVA with a Tukey multiple comparisons test using the same software.

### Digital microscopy

Selected samples ( $N = 4$ ) were examined using a digital microscopy/3D surface profilometry system, Keyence VHX-1000 with a VH-Z25 lens with optical magnification from  $\times 100$  to  $1000\times$ . Images were acquired by scanning the image plane of the microscope and reconstructing a depth composition image with all points at optimum focal points displayed in a 2D image.

## RESULTS

### OCT

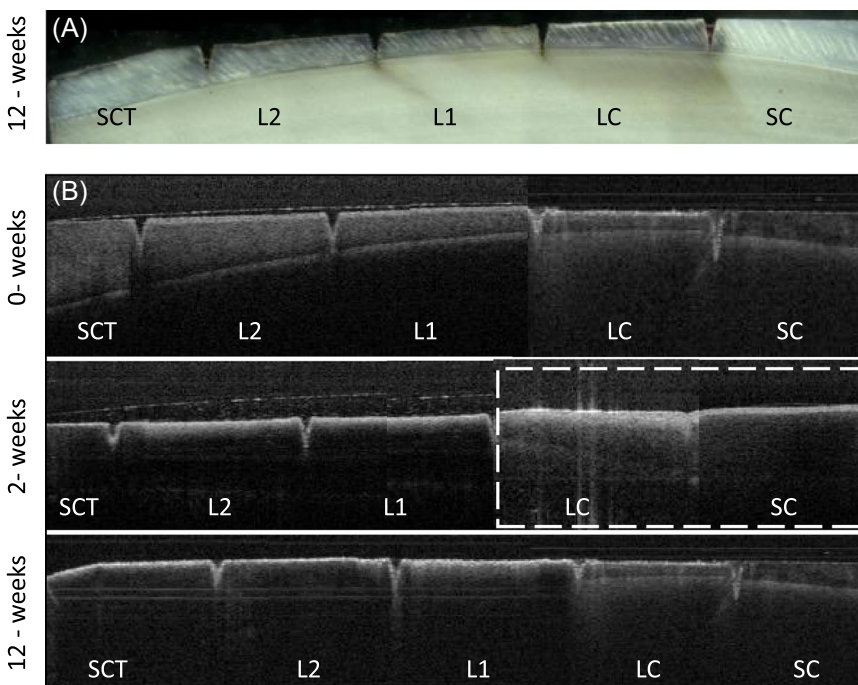
#### Enamel

A series of OCT b-scan images taken across one of the bovine enamel samples are shown in Figure 3 taken at 0, 2, and 12 weeks, along with a high-resolution microscope image of a cross-section cut from one of the samples. In sound areas, the initial OCT images before application of SDF show a narrow high-intensity peak at the position of the enamel surface representing the surface reflection followed by weak reflectivity from the underlying sound enamel with a subsequent second peak at the position of the dental enamel junction (DEJ). In the lesion areas, there is a wider peak representing the surface reflection and the increased reflectivity from the lesions that are approximately 100  $\mu\text{m}$  deep. The higher reflectivity of the lesion areas also reduces OP to the underlying DEJ and thus the DEJ has reduced visibility in lesion areas. After application of SDF in sound areas the amplitude and width of the peak representing the surface reflection broadened and the intensity increased indicating that the SDF is deposited in-depth and is not localized to the surface. The SDF also reduces OP and the subsurface reflectivity and the visibility of the underlying DEJ is greatly reduced. In the lesion areas, the SDF did not markedly change the intensity and width of the peak representing the lesion, however, it further reduced OP through the lesion and prevented resolution of the underlying DEJ. After 12 weeks the DEJ can only be seen in the windows in which SDF was not applied, LC and SC, while at 0 weeks the DEJ is visible in all five windows.

The mean intensity of the first peak along with the mean width (PW) representing the lesion and SDF are plotted in Figure 4 for the SCT, L1, and L2 windows for 0 through 12 weeks.

For the SCT, the mean intensity increased significantly after the first week and then it decreased over time with a slightly increased intensity after 12 weeks.

**FIGURE 3** (A) Digital microscopy image of a thin section cut from one of the enamel bovine block samples. Windows from the left, sound control test SCT, lesion with two applications L2, lesion with one application L1, control lesion LC and sound control SC. (B) Stitched OCT b-scans taken across a sample at 0, 2, and 12 weeks after SDF application. There is acid-resistant varnish on the surface of the LC and SC windows for week 2 (dashed box). The dentinal enamel junction (DEJ) disappears after the application of SDF due to reduced optical penetration. SDF, silver diamine fluoride



The intensity dropped rapidly from Week 3 to Week 4 and then recovered rapidly from Week 4 to 7. For the L1, L2 windows there was similar behavior, however, there was no increase in intensity after the first week.

The SCT, L1, and L2 windows all showed an increase in peak width 1 week after application of SDF. PW subsequently decreased over time after Week 1 and returned to a similar thickness for L1 and L2 while it was still significantly thicker for the SCT window.

The OP, that is, the intensity at  $180\ \mu\text{m}$  below the surface is also plotted in Figure 4 for the SCT, L1, and L2 windows for 0 through 12 weeks. For enamel, the intensity dropped markedly after application of SDF in a similar fashion for the SCT, L1, and L2 windows and continued to decrease up to 4 weeks where it remained significantly lower after the 12 weeks.

## Dentin

A series of OCT b-scan images taken across all five windows of one of the bovine dentin samples are shown in Figure 5 taken at 0, 2, and 12 weeks along with a high-resolution microscope image of a cross-section cut from one of the samples. Both sound and demineralized dentin strongly scatter SWIR light. The scattering of demineralized dentin is only slightly stronger than sound dentin. In both sound and lesion areas, the initial OCT images before application of SDF show a broad high-intensity peak at the position of the dentin surface with much less OP than is observed for enamel. In the lesion areas, the intensity is only slightly higher. After application of SDF, there is a large increase in the intensity with

marked narrowing of the peak width. The deposition of the highly scattering SDF increases the reflectivity and greatly reduces the peak width. In contrast to enamel, SDF application increased the reflectivity from deeper layers in the dentin.

The mean intensity of the first peak along with the mean PW due to the lesion and SDF are plotted in Figure 4 for the SCT, L1, and L2 windows for 0 through 12 weeks. All three windows showed similar behavior with time. The mean intensity increased significantly only after the first week and then it decreased gradually over time with a slightly increased intensity after 12 weeks. There was no significant difference ( $p > 0.05$ ) between the three windows for the mean intensity (ANOVA) before the application of SDF. Lesion windows with SDF are significantly different ( $p < 0.05$ ) from control windows after 12 weeks. The mean intensity was significantly ( $p < 0.05$ ) higher after 12 weeks than before SDF application for SCT, L1, and L2 windows (RM-ANOVA). Lesion windows (L1, L2) showed a significant difference ( $p < 0.05$ ) when compared with the control lesion over the 12 weeks after SDF was applied. The second application after Week 6 on L2 had no apparent effect on the mean intensity.

Changes in the peak width also showed similar behavior with time for all three windows. The width decreased markedly after the application of SDF for the lesion and sound windows for the first 2 weeks after SDF application. The peak width remained fairly constant until the 10th week where there was a slight non-significant increase for Week 12. After 12 weeks the peak width was significantly lower ( $p < 0.05$ ) than at Week 0. The second application after Week 6 on L2 had no apparent effect on the peak width.

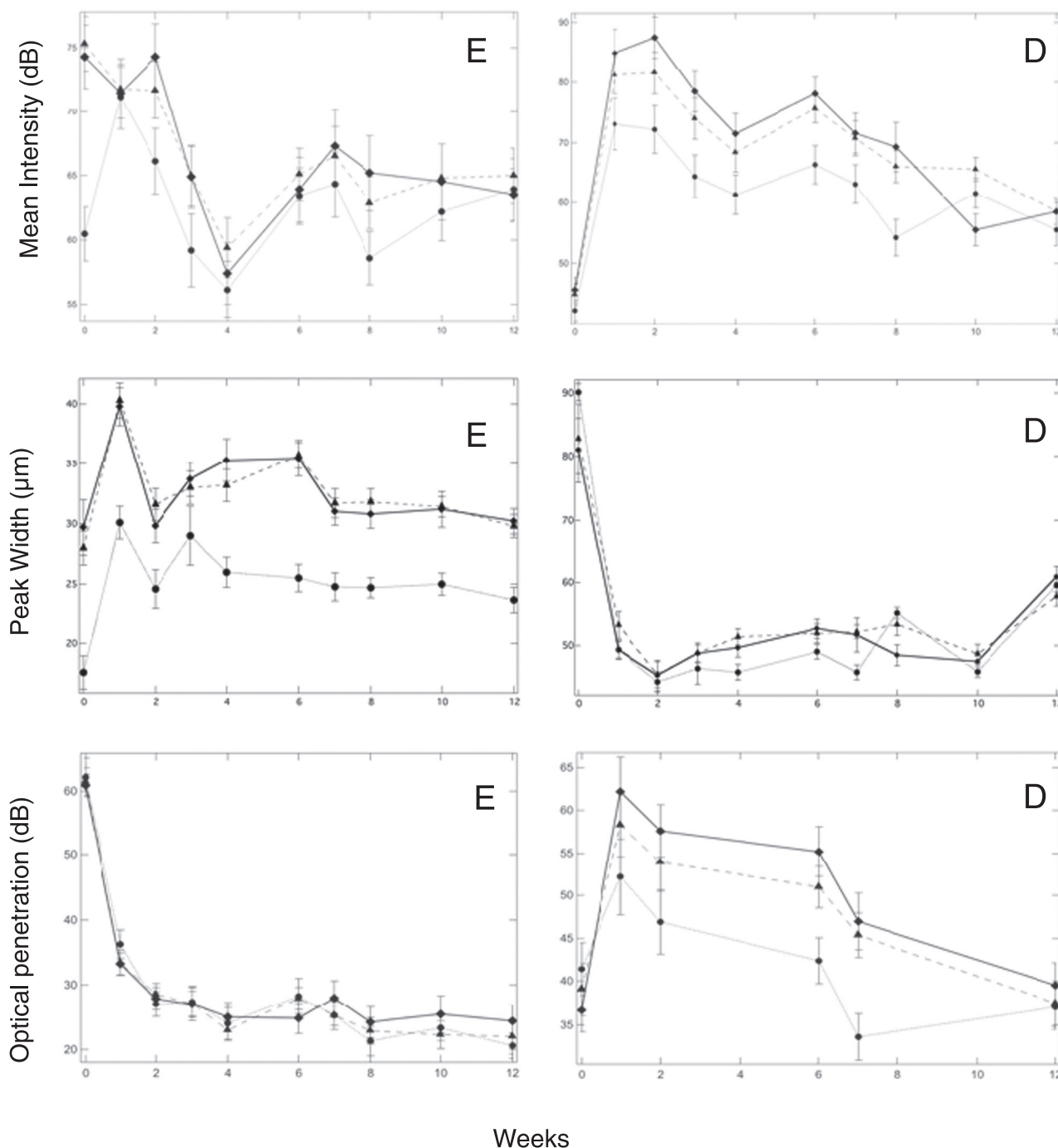


**FIGURE 4** Graphs of the mean ( $\pm$ SEM) peak intensity and width (intensity and width of the surface and lesion areas shown in Figure 2) and mean ( $\pm$ SEM) intensity at a depth of  $180\ \mu\text{m}$  from the surface (optical penetration) for the SCT, L1 and L2 enamel (E) and dentin (D) windows. The circles and thin dotted line, the triangles and dashed line, and the diamonds and solid line represent the SCT, L1, and L2 windows, respectively

The OP, that is, the intensity at  $180\ \mu\text{m}$  below the surface shows a very different behavior with time than for enamel as can be seen in Figure 4. For dentin, the intensity of the sound and lesion windows increased markedly after application of SDF in a similar fashion for the SCT, L1, and L2 windows and subsequently decreased back to a similar intensity to Week 0 after 12 weeks.

### Thermal imaging dehydration measurements

Thermal images at different time points and temperature versus time profiles for individual sound and lesion windows are shown in Figures 6 and 7 before and after SDF application. In the lesion areas, there is a larger drop in temperature during drying yielding a larger increase in  $\Delta Q$  due to evaporative cooling in the



**FIGURE 5** (A) Digital microscopy image of a thin section cut from one of the dentin bovine block samples. Windows from the left, sound control test SCT, lesion with two applications L2, lesion with one application L1, control lesion LC and sound control SC. (B) Stitched OCT b-scans taken across a sample at 0, 2, and 12 weeks after SDF application. There is acid-resistant varnish on the surface of the LC and SC windows for Week 2 (dashed box). OCT, optical coherence tomography

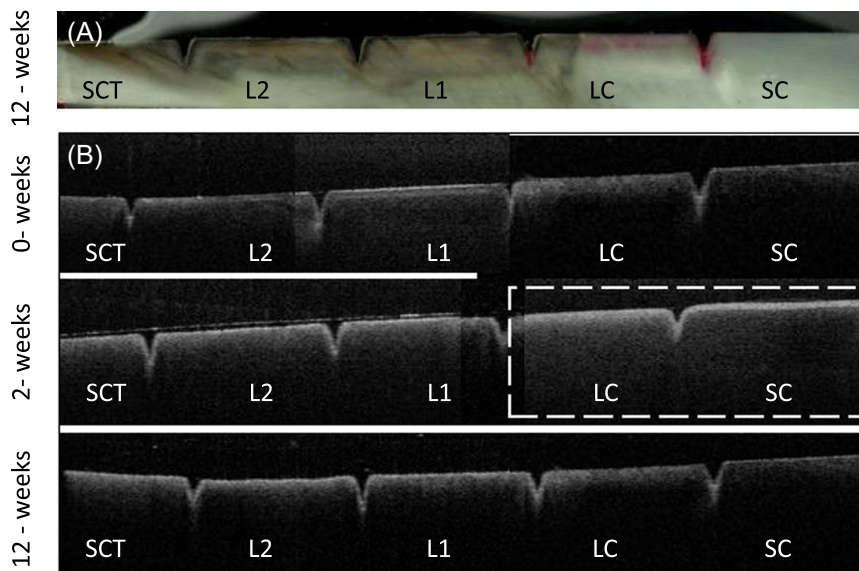
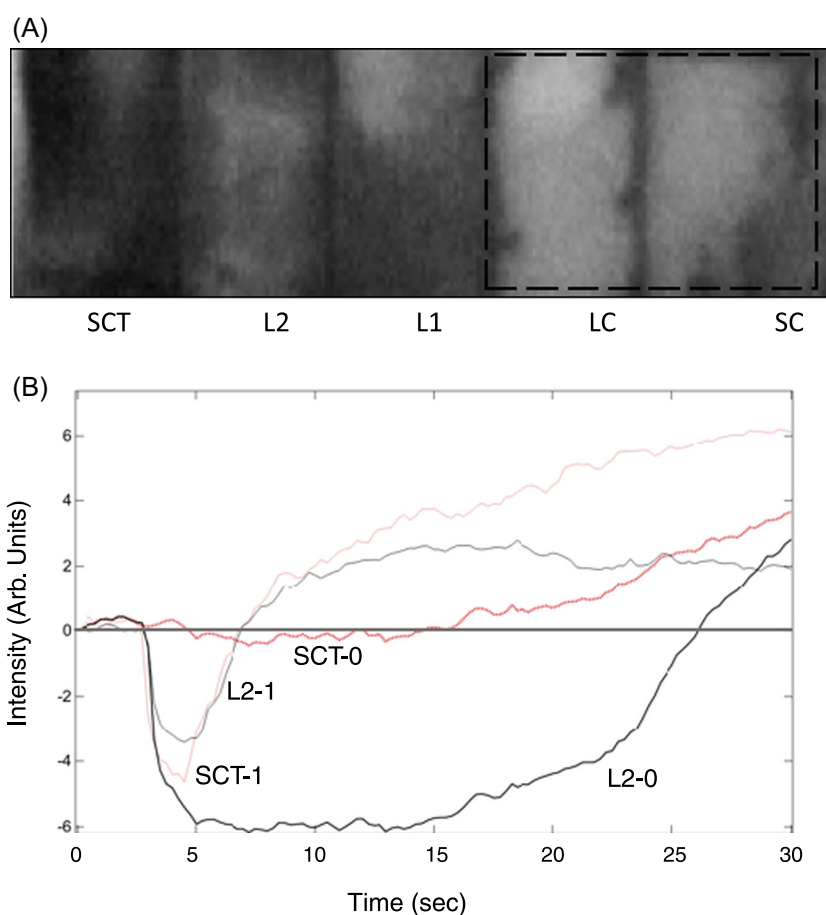


**FIGURE 6** (A) Thermal image of one of the enamel blocks after 5 seconds of drying, cooler areas are darker and the LC and SC windows (dashed box) are covered with acid-resistant varnish. (B) Curves of the measured temperature (thermal emission) versus time from the surface of the SCT and L2 windows at 0 and 1 week after SDF application are shown for one of the samples. DQ values represent the area under the curves representing the temperature drop during drying, that is, the area under the gray line at zero. LC, lesion control; SC, sound control; SCT, serve as a test control; SDF, silver diamine fluoride



higher porosity areas of the lesion compared to sound areas.

The thermal image shown in Figure 6 taken after 5 seconds of drying an enamel sample shows that the SCT, L1, and L2 windows are darker than the LC and SC windows that are covered with varnish. This indicates

that they are cooler due to the loss of water from the more porous windows. Time versus temperature curves are also shown at 0 and 1 week for the SCT and L2 windows. One week after SDF application, the thermal profile significantly changed and shows a lower drop and faster recovery while for the SCT window the opposite

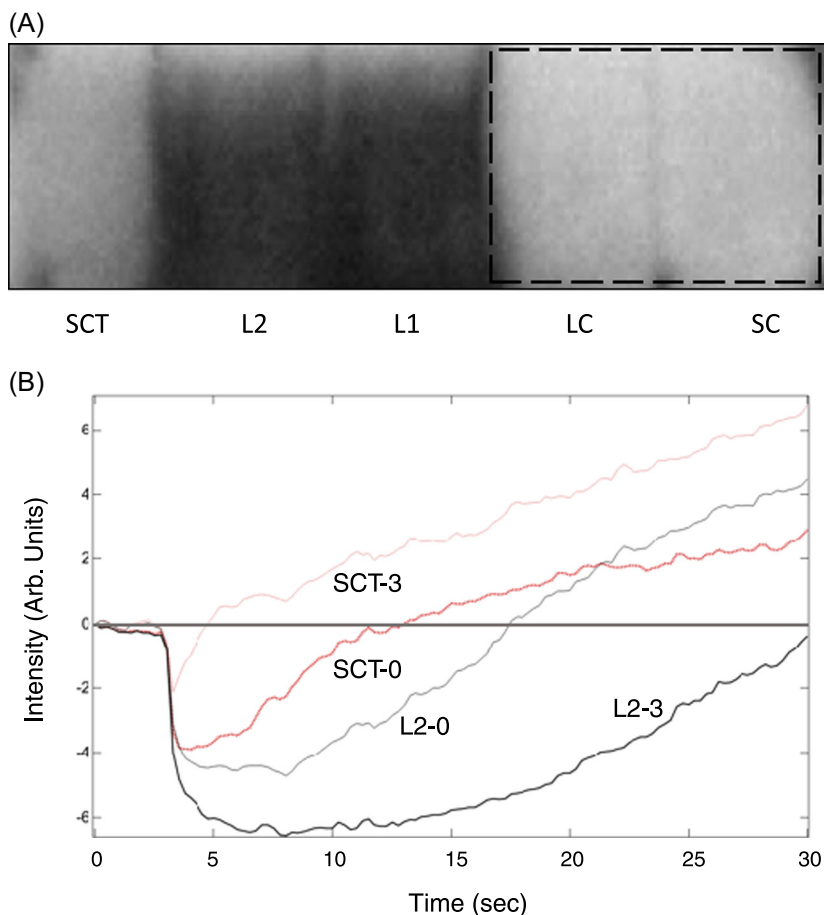


**FIGURE 7** (A) Thermal image of one of the dentin blocks after 10 seconds of drying. The LC and SC windows (dashed box) are covered with acid-resistant varnish. (B) Curves of the measured temperature (thermal emission) versus time from the surface of the SCT and L2 windows at 0 and 3 weeks after SDF application are shown for one of the samples. LC, lesion control; SC, sound control; SCT, serve as a test control; SDF, silver diamine fluoride

occurred, there is a larger drop and greater area under zero or  $\Delta Q$ .  $\Delta Q$  is plotted in Figure 8 for enamel and dentin for the SCT, L1, and L2 windows for 0 through 12 weeks.

Adding SDF to sound enamel increased the  $\Delta Q$  significantly over the first 3 weeks then it gradually returned to normal after 12 weeks. However, the  $\Delta Q$  values for L1 and L2 continually decreased for the first 8 weeks and were significantly lower than Week 0 after 12 weeks. When comparing the 5 windows on Week 12, SDF treated windows (L1, L2) were significantly different from the control lesion (LC). The control window with SDF (C W12) was not significantly different from the sound control window (SC).

A thermal image shown in Figure 7 taken after 10 seconds of drying a dentin sample shows that the L1 and L2 windows are darker than the SCT, LC, and SC windows. The difference perceived between the sound and lesion windows after SDF application was not observed for dentin. For dentin, the sound and lesion windows behaved similarly over time.  $\Delta Q$  increased significantly for the first 4 weeks and subsequently returned to its initial values after 6 weeks resulting in no significant difference in  $\Delta Q$  between Week 0 and Week 12 for the SCT, L1, and L2 windows.

### Mineral density measurements on enamel and dentin

Even though the values measured showed the expected trend, where the lesion windows had lower mineral density values. Statistical analysis of the mineral density measured at the surface (lesion layer) on each window showed no significant differences between the five windows on enamel or dentin (ANOVA).

### Digital microscopy

Figure 9 shows cross-sections cut from the samples 12 weeks after SDF application along with images of enamel and dentin surfaces 1 day and 4 weeks after SDF application. High magnification images of dentin show that the precipitation of SDF has occurred in-depth and has occluded the dentinal tubules, while images of the enamel surface show that SDF precipitation is limited to a thin layer at the enamel surface.

On the dentin, windows discoloration is visible on the treated sound and lesion windows. The lesion areas in the cross-section show darker discoloration indicative of silver precipitation within the lesion body. Discoloration

**FIGURE 8** Graphs of the mean ( $\pm$ SEM) values of DQ for the (E) and dentin (D) windows from 0 to 12 weeks. The circles and thin dotted line, the triangles and dashed line and the diamonds and solid line represent the SCT, L1, and L2 windows, respectively

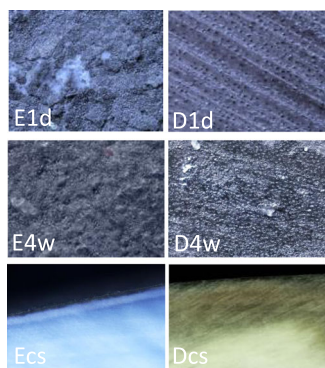
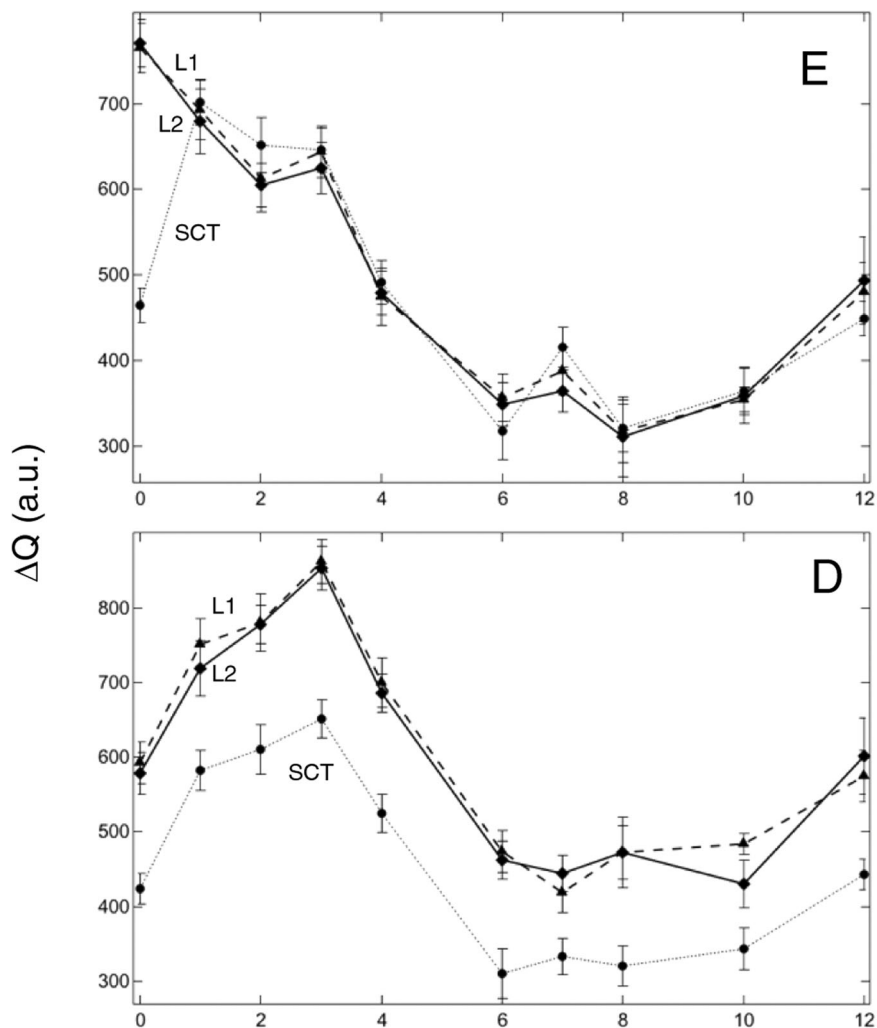


**FIGURE 9** Digital microscopy images of enamel (E) and dentin (D) surfaces after 1 day of SDF application (1 d) and after 4 weeks (4 w) of SDF application ( $\times 900$ ). Cross-sectional images (cs) of the sectioned enamel and dentin bovine blocks ( $\times 500$ ) showing SDF precipitate remaining on the surface of enamel and subsurface staining 12 weeks after SDF application. SDF, silver diamine fluoride

extends in depth below the dentin lesions indicating that silver particles can infiltrate deep into the dentin. Enamel cross-sections show a well-defined dark layer on the surface of sound and lesion windows indicative of SDF

precipitation. Discoloration of the surface of the control lesion happened after removing the nail varnish.

### DISCUSSION

In this study, we observed for the first time the behavior of SDF over time using OCT and thermal imaging. We observed that SDF deposits silver metal during treatment of caries lesions and that deposition changes the surface and subsurface reflectivity measured with OCT.

After application of SDF on the surface of enamel and dentin bovine blocks, a significant increase in the intensity (reflectivity) of the surface layer can be observed. The deposition of silver metal, highly reflective at 1300 nm, is responsible for this layer.

OCT images of sound enamel typically show a sharp peak at the sample surface followed by a layer of weak reflectivity from the internal sound enamel. The reflectivity increases at the dentinal enamel junction due to the higher reflectivity of dentin producing a second peak (Figure 2). The reflectivity of demineralized enamel is

orders of magnitude higher than sound enamel and demineralized enamel shows up with high contrast compared to sound enamel in OCT images. OCT images of dentin are quite different as the scattering of sound dentin is much higher than for sound enamel due to the strong scattering by dentinal tubules. It is more difficult to differentiate sound and demineralized dentin and the overall OP is reduced to 1–2 mm for dentin while the OP is much greater in enamel and studies have shown that lesions (e.g., approximal lesions) can be imaged through 4–5 mm of sound enamel.<sup>38</sup> After the application of SDF on the surface of sound enamel bovine blocks, there was a significant increase in the intensity (reflectivity) and the width of the primary peak in the OCT images suggesting that SDF was deposited on and penetrated the surface of enamel. High-resolution microscopy confirmed that the SDF was deposited on the surface and penetrated into sound enamel in addition to the deeper penetration observed in lesion areas. The application of SDF also showed the classic change in color that had been observed clinically due to the deposition of silver as can be seen in Figures 1 and 9.<sup>4,39</sup> The deposition of the SDF in lesion areas resulted in a decrease in the intensity of reflectivity/scattering from the lesion areas suggesting that the SDF resulted in some filling of the pores over the 12-week period.

SDF deposition resulted in a marked decrease in the subsurface reflectivity both in sound and lesion areas for enamel. This suggests that the silver is blocking OP in addition to increasing the reflectivity. Remineralization of the enamel lesions would be expected to both reduce the mean intensity and reduce the peak width representing the lesion depth while increasing OP through the lesion, that is, increasing the intensity at a depth of 180  $\mu\text{m}$ . Since the opposite occurs, we cannot conclude that remineralization of the lesion has taken place even though the intensity of the reflectivity from lesion areas has decreased after 12 weeks. The SDF appears to have formed a thin surface barrier since the intensity well below the surface decreased significantly and did not recover. Decreases in the intensity after SDF application in both sound and lesion areas enamel suggests that the silver particles leach out over time.

The changes observed on dentin in the OCT images after SDF application varied greatly from those observed for enamel. The intensity and width of the peak was similar on all the windows before application of SDF. The intensity rapidly increased during the first 2 weeks which is consistent with the deposition of silver throughout the tubules in both the sound and lesion windows. Silver likely leaked into the solution of artificial saliva over time which may explain the attenuation of the intensity values over the 12 weeks period. This leaking may also explain the staining we noticed on the control windows after the removal of nail polish for the final measurements when the samples were put back into a new solution.

SDF deposition also produced a marked reduction in the peak width on the dentin samples after the first 2 weeks that was maintained throughout the entire 12 weeks. Contrary to expectations, the intensity increased at a depth of 180  $\mu\text{m}$  after the application of SDF for the first 2 weeks then gradually went back to normal after 12 weeks. It is likely that the silver penetrated much further into the dentin than in the enamel and that in the case of dentin there was the substantial deposition of silver at a depth of 180  $\mu\text{m}$  increasing the reflectivity. The silver particles appear to both enhance reflectivity, that is, act as a contrast enhancer<sup>40</sup> and block OP to deeper layers underneath. In the case of enamel, the silver did not penetrate to 180  $\mu\text{m}$ , therefore the higher density layer of silver particles blocked OP while there was no enhancement of the reflectivity by the silver at a depth of 180  $\mu\text{m}$ . OCT studies with silver and titanium nanoparticles indicate such particles can act as contrast enhancers.<sup>40,41</sup> The reduction of the intensity at 180  $\mu\text{m}$  with time may be attributed to the silver moving out of the tubules with time. The discoloration found on the cross-sections examined under high magnification (Figure 9) penetrated much deeper than 180  $\mu\text{m}$  in dentin which supports this theory.

Thermal imaging indicated a rapid increase in  $\Delta Q$  after application of SDF on sound enamel. This can be explained by the deposition of a rough porous precipitate on the surface. Cross-sectional images show a rough precipitate on the enamel surface and that precipitate may dissolve with time. The formation of a precipitate can explain increases in the peak intensity and width along with the decrease in the apparent OP in the OCT images along with the increase in  $\Delta Q$ .

Another possible explanation is that the SDF and silver deposition change the emissivity of the enamel surface. Metals have lower emissivity so it would not be surprising if the emissivity dropped significantly after SDF application however a decline in emissivity would lower  $\Delta Q$  not raise it. Moreover, the emissivity of dental hard tissues is high, Enamel was recently measured to be 0.96, and dentin was measured to be 0.92 so a substantial increase in emissivity would not be possible.<sup>42</sup> To investigate the influence of SDF on the emissivity, SDF was applied to a tooth surface and a tongue depressor and allowed to dry. The SDF did not change the temperature on these samples.

The thermal imaging measurements on dentin indicated that demineralized and sound dentin behaved similarly.  $\Delta Q$  increased significantly during the first 4 weeks and then subsequently gradually returned to its initial value before SDF application after 12 weeks. The same behavior was observed on sound enamel. However, enamel lesions showed the opposite behavior with a decrease in  $\Delta Q$  value over time and a slight increase toward 12 weeks. A reduction of  $\Delta Q$  is indicative of decreased permeability and lesion arrest. On enamel, the results can be explained by the formation of a distinct layer of silver on the lesion surface

as well as silver infiltration within the lesion which leads to reduced lesion permeability. However, for dentin, it seems as if the lesion became more active during the first 4 weeks, and then  $\Delta Q$  only dropped after 4 weeks. The values seem to return to baseline before SDF application by the end of 12 weeks. Meaning that even if the SDF did affect the permeability of the dentin lesions, the effect was not significant after 12 weeks.

Observed differences in behavior between enamel and dentin can be explained by the structural characteristics of the two tissues. Enamel is significantly more mineralized and less porous than dentin. Under high optical magnification (Figure 9), it was observed that during the precipitation of SDF on dentin, the tubules were occluded by the precipitation of the SDF, while on enamel surfaces a well-defined surface layer was formed. Typical silver staining on sample sections followed structural cues in the tissue. For dentin, the staining followed the direction of the tubules and in enamel, the staining is mainly localized to the surface. Lesions were stained dark black, yet lighter brown staining was observed to extend further than the lesions themselves and even further than where the silver particles were detected using optical microscopy. This can be due to the diffusion of residual SDF within the tubules. Yamaga et al.<sup>43</sup> concluded that the black staining on SDF-treated tooth surfaces was due to the formation of  $\text{Ag}_3\text{PO}_4$ . Mei et al.<sup>32</sup> suggested that silver compounds are the reason for the black staining. In fact, the presence of oxygen, phosphorus, and sulfur as well as increased chlorine in the SDF-treated carious lesions suggests that these elements can incorporate into silver and form not only  $\text{Ag}_3\text{PO}_4$ , but also variants of silver oxide ( $\text{AgO}$ ,  $\text{Ag}_2\text{O}$ , or  $\text{Ag}_4\text{O}_4$ ) and silver sulfide ( $\text{Ag}_2\text{S}$ ). The transition from silver ions ( $\text{Ag}^+$ ) to metallic silver particles ( $\text{AgO}$ ,  $\text{Ag}_2\text{O}$ ,  $\text{Ag}_4\text{O}_4$ ) contributes to the black staining resulting from SDF application on the surface of carious lesions.<sup>44</sup> There was also a slight difference in penetration depth on the treated windows. On four of the five sectioned samples, the staining depth on sample regions/windows treated twice (both at 0 and 6 weeks) was less than the depth with one treatment. Reduced permeability after the second application may explain this finding. It appears that residual SDF may remain mobile inside the tubules. This may also depend on mineral content, the staining on healthy dentin seemed to be less severe than for the demineralized dentin. It is likely that the stained tubules were filled with silver particles that eventually “leaked” out with time. This theory can explain changes observed with OCT and thermal imaging over time. A further investigation comparing OCT signals and the amount of precipitated silver observed in the tubules after each week after SDF application might confirm such behavior.

A second application of SDF on the same samples after 6 weeks had little effect on OCT and thermal imaging measurements. We believe that since our lesions were shallow (around 80–100  $\mu\text{m}$  in-depth) the second

application of SDF had no effect on the plugged tubules in dentin or the superficial layer formed on enamel.

TMR results obtained on five sectioned dentin blocks show the expected trend in values. The sound control and sound test windows have the highest mineral content, the control lesions had the lowest and the two treated lesion windows show slightly higher values which indicate a higher degree of remineralization. Additional studies should consider doing TMR measurements early after the initial SDF application to provide information about initial events leading up to remineralization.

This manuscript introduces two novel methods for monitoring changes in the lesions over time, OCT and thermal imaging both of which show changes in the light scattering and permeability of caries lesions after treatment. The signals observed in this study (OCT reflectivity and thermal changes due to modification of permeability) can be considered indicators of lesion activity. It must be kept in mind that it is not possible to interpret the overall effect of SDF on carious lesions based solely on our *in vitro* results. *In vivo* the efficacy of SDF may be different due to the oral hygiene of the patient and SDF's antibacterial activity, however, such differences should not interfere with the ability of these methods to monitor lesions in the clinic. For example, the amount of silver “leaking” from the lesion after 12 weeks may still be enough to affect the bacteria, but not enough to enhance the mineral content/behavior detected here.

## CONCLUSION

For the first time, we demonstrate that changes in simulated caries lesions on enamel and dentin can be monitored after applying SDF using thermal and OCT imaging. Measurements were made over 12 weeks after SDF application and showed significant changes in reflectivity, OP, and permeability in both sound and demineralized enamel and dentin. High-resolution microscopy images confirmed structural changes in enamel and dentin after SDF application. Such changes can potentially be monitored to determine if and when reapplication of SDF is needed.

## ACKNOWLEDGMENTS

This project was mainly supported by the Swiss National Science Foundation SNSF and achieved during a PostDoc program at the University of California UCSF under the supervision of Pr. Fried. Swiss National Science Foundation (SNSF), Switzerland. (Grant ID: P2GEP3\_188157). NIH grants R01-DE027335 and F30-DE027264. Open access funding provided by Universite de Geneve.

## CONFLICT OF INTERESTS

The authors declare that there are no conflicts of interest.

## ORCID

Marwa Abdelaziz  <https://orcid.org/0000-0002-9715-879X>

Daniel Fried  <https://orcid.org/0000-0002-5327-2558>

## REFERENCES

1. Stebbins EA. What value has argenti nitras as a therapeutic agent in dentistry? *Int Dent J*. 1891;12:661–70.
2. Gao SS, Zhao IS, Hiraishi N, Duangthip D, Mei ML, Lo ECM, et al. Clinical trials of silver diamine fluoride in arresting caries among children: a systematic review. *JDR Clin Trans Res*. 2016; 1(3):201–10.
3. Fung MHT, Duangthip D, Wong MCM, Lo ECM, Chu CH. Randomized clinical trial of 12% and 38% silver diamine fluoride treatment. *J Dent Res*. 2018;97(2):171–8.
4. Horst JA, Ellenikiotis H, Milgrom PL. UCSF protocol for caries arrest using silver diamine fluoride: rationale, indications and consent. *J Calif Dent Assoc*. 2016;44(1):16–28.
5. Rosenblatt A, Stamford T, Niederman R. Silver diamine fluoride: a caries "Silver-Fluoride Bullet". *J Dent Res*. 2009;88(2):116–25.
6. Chu CH, Lo EC, Lin HC. Effectiveness of silver diamine fluoride and sodium fluoride varnish in arresting dentin caries in Chinese pre-school children. *J Dent Res*. 2002;81(11):767–70.
7. Mei ML, Ito L, Cao Y, Lo EC, Li QL, Chu CH. An ex vivo study of arrested primary teeth caries with silver diamine fluoride therapy. *J Dent*. 2014;42(4):395–402.
8. Chu CH, Lo EC. Microhardness of dentine in primary teeth after topical fluoride applications. *J Dent*. 2008;36(6):387–91.
9. Mei ML, Chu CH, Low KH, Che CM, Lo EC. Caries arresting effect of silver diamine fluoride on dentine carious lesion with *S. mutans* and *L. acidophilus* dual-species cariogenic biofilm. *Med Oral Patol Oral Cir Bucal*. 2013;18(6):e824–31.
10. Mei ML, Ito L, Cao Y, Li QL, Lo EC, Chu CH. Inhibitory effect of silver diamine fluoride on dentine demineralisation and collagen degradation. *J Dent*. 2013;41(9):809–17.
11. Wierichs RJ, Stausberg S, Lausch J, Meyer-Lueckel H, Esteves-Oliveira M. Caries-preventive effect of NaF, NaF plus TCP, NaF plus CPP-ACP, and SDF varnishes on sound dentin and artificial dentin caries in vitro. *Caries Res*. 2018;52(3):199–211.
12. Fried D, Xie J, Shafi S, Featherstone JD, Breunig TM, Le C. Imaging caries lesions and lesion progression with polarization sensitive optical coherence tomography. *J Biomed Opt*. 2002;7(4):618–27.
13. Amaechi BT, Higham SM, Podoleanu AG, Rogers JA, Jackson DA. Use of optical coherence tomography for assessment of dental caries: quantitative procedure. *J Oral Rehabil*. 2001; 28(12):1092–3.
14. Can AM, Darling CL, Fried D. High-resolution PS-OCT of enamel remineralization. *Proc SPIE Int Soc Opt Eng*. 2008;6843: 68430T68431–7.
15. Fried D, Staninec M, Darling CL, Chan KH, Pelzner RB. Clinical monitoring of early caries lesions using cross polarization optical coherence tomography. *Proc SPIE Int Soc Opt Eng*. 2013;8566: 856604.
16. Lee C, Darling C, Fried D. Polarization sensitive optical coherence tomographic imaging of artificial demineralization on exposed surfaces of tooth roots. *Dent Mat*. 2009;25(6):721–8.
17. Manesh SK, Darling CL, Fried D. Nondestructive assessment of dentin demineralization using polarization-sensitive optical coherence tomography after exposure to fluoride and laser irradiation. *J Biomed Mater Res B Appl Biomater*. 2009;90(2):802–12.
18. Manesh SK, Darling CL, Fried D. Polarization-sensitive optical coherence tomography for the nondestructive assessment of the remineralization of dentin. *J Biomed Opt*. 2009;14(4):044002.
19. Chan KH, Fried D. Multispectral cross-polarization reflectance measurements suggest high contrast of demineralization on tooth surfaces at wavelengths beyond 1300-nm due to reduced light scattering in sound enamel. *J Biomed Opt*. 2018;23(6):060501-4.
20. Chan KH, Tom H, Lee RC, Kang H, Simon JC, Staninec M, et al. Clinical monitoring of smooth surface enamel lesions using CP-OCT during nonsurgical intervention. *Lasers Surg Med*. 2016; 48(10):915–23.
21. Louie T, Lee C, Hsu D, Hirasuna K, Manesh S, Staninec M, et al. Clinical assessment of early tooth demineralization using polarization sensitive optical coherence tomography. *Lasers in Surg Med*. 2010;42:738–45.
22. Nee A, Chan K, Kang H, Staninec M, Darling CL, Fried D. Longitudinal monitoring of demineralization peripheral to orthodontic brackets using cross polarization optical coherence tomography. *J Dent*. 2014;42(5):547–55.
23. Staninec M, Douglas SM, Darling CL, Chan K, Kang H, Lee RC, et al. Nondestructive clinical assessment of occlusal caries lesions using near-IR imaging methods. *Lasers Surg Med*. 2011;43(10): 951–9.
24. Chu CH, Lee AH, Zheng L, Mei ML, Chan GC. Arresting rampant dental caries with silver diamine fluoride in a young teenager suffering from chronic oral graft versus host disease post-bone marrow transplantation: a case report. *BMC Res Notes*. 2014;7:3.
25. Ando M, Ferreira-Zandona AG, Eckert GJ, Zero DT, Stookey GK. Pilot clinical study to assess caries lesion activity using quantitative light-induced fluorescence during dehydration. *J Biomed Opt*. 2017;22(3):35005.
26. Lee RC, Darling CL, Fried D. Assessment of remineralization via measurement of dehydration rates with thermal and near-IR reflectance imaging. *J Dent*. 2015;43:1032–42.
27. Lee RC, Staninec M, Le O, Fried D. Infrared methods for assessment of the activity of natural enamel caries lesions. *IEEE J Sel Top Quantum Electron*. 2014;22(3):6803609.
28. Lee RC, Darling CL, Staninec M, Ragadio A, Fried D. Activity assessment of root caries lesions with thermal and near-IR imaging methods. *J Biophotonics*. 2017;10(3):433–45.
29. Kaneko K, Matsuyama K, Nakashima S. Quantification of early carious enamel lesions by using an infrared camera in vitro. In: Stookey GK, editor. Early detection of dental caries. II. Proc 4th Annu Indiana Conf, Indianapolis, Indiana University School of Dentistry, 2000. pp. 83–99.
30. Zakian CM, Taylor AM, Ellwood RP, Pretty IA. Occlusal caries detection by using thermal imaging. *J Dent*. 2010;38(10):788–95.
31. Yang V, Zhu Y, Curtis D, Le O, Chang N, Fried W, et al. Thermal imaging of root caries in vivo. *J Dent Res*. 2020;99(13): 1502–8.
32. Mei ML, Lo ECM, Chu CH. Arresting dentine caries with silver diamine fluoride: what's behind it? *J Dent Res*. 2018;97(7):751–8.
33. Seto J, Horst JA, Parkinson DY, Frachella JC, DeRisi JL. Enhanced tooth structure via silver microwires following treatment with 38 percent silver diamine fluoride. *Pediatr Dent*. 2020;42(3): 226–31.
34. Mellberg JR. Hard-tissue substrates for evaluation of cariogenic and anti-cariogenic activity in situ. *J Dent Res*. 1992;71(3):913–9.
35. Yamazaki H, Litman A, Margolis HC. Effect of fluoride on artificial caries lesion progression and repair in human enamel: regulation of mineral deposition and dissolution under in vivo-like conditions. *Arch Oral Biol*. 2007;52(2):110–20.
36. Wang RK, Elder JB. Propylene glycol as a contrasting agent for optical coherence tomography to image gastrointestinal tissues. *Lasers Surg Med*. 2002;30(3):201–8.
37. Darling CL, Featherstone JDB, Le CQ, Fried D. An automated digital microradiography system for assessing tooth demineralization. *Proc SPIE Int Soc Opt Eng*. 2009;7162(1):71620T.
38. Shimada Y, Burrow MF, Araki K, Zhou Y, Hosaka K, Sadr A, et al. 3D imaging of proximal caries in posterior teeth using optical coherence tomography. *Sci Rep*. 2020;10(1):15754.
39. Milgrom P, Horst J, Ludwig S, Rothen M, Chaffee B, Lyalina S, et al. Topical silver diamine fluoride for dental caries arrest in pre-school children: a randomized controlled trial and microbiological

- analysis of caries associated microbes and resistance gene expression. *J Dent.* 2018;68:72–8.
40. Vanda SM, Carneiro CCBOM, Souza AF, da Silva EJ, da Silva AF, Gerbi MEMM, et al. Silver nanoparticles as optical clearing agent enhancers to improve caries diagnostic by optical coherence tomography. In: *Proc SPIE 10507, colloidal nanoparticles for biomedical applications XIII*; 2018. p. 1050719.
  41. Braz AKS, Moura DS, Gomes ASL, Ohulchanskyy TY, Chen G, Liu M, et al. TiO<sub>2</sub>-coated fluoride nanoparticles for dental multimodal optical imaging. *J Biophotonics.* 2018;11(4): e201700029.
  42. Soori A, Kowsary F, Kasraei S. Experimental estimation of the emissivity of human enamel and dentin. *Infrared Phys Technol.* 2020;106:103234.
  43. Yamaga R, Nishino M, Yoshida S, Yokomizo I. Diammine silver fluoride and its clinical application. *J Osaka Univ Dent Sch.* 1972; 12:1–20.
  44. Li Y, Liu Y, Psoter WJ, Nguyen OM, Bromage TG, Walters MA, et al. Assessment of the silver penetration and distribution in carious lesions of deciduous teeth treated with silver diamine fluoride. *Caries Res.* 2019;53(4):431–40.

**How to cite this article:** Abdelaziz M, Yang V, Chang N-YN, Darling C, Fried W, Seto J, et al. Monitoring silver diamine fluoride application with optical coherence tomography and thermal imaging: an in vitro proof of concept study. *Lasers Surg Med.* 2022;54:790–803.  
<https://doi.org/10.1002/lsm.23528>